Sustained regression of tumors upon MYC inactivation requires p53 or thrombospondin-1 to reverse the angiogenic switch

Sylvie Giuriato*†, Sandra Ryeom‡, Alice C. Fan*, Pavan Bachireddy*, Ryan C. Lynch‡, Matthew J. Rioth‡, Jan van Riggelen*, Andrew M. Kopelman*, Emmanuelle Passegué§¶, Flora Tang*, Judah Folkman‡, and Dean W. Felsher*‖

*Departments of Medicine and Pathology, Division of Oncology, Stanford University School of Medicine, CCSR Building, Room 1120, 269 Campus Drive, Stanford, CA 94305-5151; ‡Department of Surgery, Vascular Biology Program, Children's Hospital Boston and Harvard Medical School, Karp 12.129, 300 Longwood Avenue, Boston, MA 02115; and §Department of Pathology, Stanford University School of Medicine, B259 Beckman Center, 279 Campus Drive, Stanford, CA 94305

Contributed by Judah Folkman, September 13, 2006

The targeted inactivation of oncogenes offers a rational therapeutic approach for the treatment of cancer. However, the therapeutic inactivation of a single oncogene has been associated with tumor recurrence. Therefore, it is necessary to develop strategies to override mechanisms of tumor escape from oncogene dependence. We report here that the targeted inactivation of MYC is sufficient to induce sustained regression of hematopoietic tumors in transgenic mice, except in tumors that had lost p53 function. p53 negative tumors were unable to be completely eliminated, as demonstrated by the kinetics of tumor cell elimination revealed by bioluminescence imaging. Histological examination revealed that upon MYC inactivation, the loss of p53 led to a deficiency in thrombospondin-1 (TSP-1) expression, a potent antiangiogenic protein, and the subsequent inability to shut off angiogenesis. Restoration of p53 expression in these tumors re-established TSP-1 expression. This permitted the suppression of angiogenesis and subsequent sustained tumor regression upon MYC inactivation. Similarly, the restoration of TSP-1 alone in p53 negative tumors resulted in the shut down of angiogenesis and led to sustained tumor regression upon MYC inactivation. Hence, the complete regression of tumor mass driven by inactivation of the MYC oncogene requires the p53-dependent induction of TSP-1 and the shut down of angiogenesis. Notably, overexpression of TSP-1 alone did not influence tumor growth. Therefore, the combined inactivation of oncogenes and angiogenesis may be a more clinically effective treatment of cancer. We conclude that angiogenesis is an essential component of oncogene addiction.

tumorigenesis | angiogenesis inhibitors

Cancers harbor multiple genetic lesions contributing to tumorigenesis through the disruption of the normal function of proto-oncogenes and/or tumor suppressor genes (1, 2). The targeted repair of these mutant gene products may be a specific and effective therapy. For example, the use of Imatinib specifically inactivates the bcr-*abl* oncogene for the treatment of chronic myelogenous leukemia (3).

The notion that tumorigenesis can be reversed through the targeted inactivation of oncogenes has been broadly demonstrated through conditional transgenic models (4, 5). Previously, we have demonstrated that inactivation of MYC can induce sustained tumor regression even in highly genomically complex and unstable hematopoietic tumors (6); furthermore, the brief inactivation of MYC can induce sustained tumor regression in some tumors (7). MYC inactivation induces a state of tumor dormancy in yet other types of cancers, such as hepatocellular carcinoma (8). Thus, tumors appear to become "addicted" to oncogenes, but the consequences of oncogene inactivation depend on the cellular and genetic context (4, 9, 10).

Cancers escape oncogene dependence by acquiring other events (6, 11–15), thus becoming resistant to oncogene inactivation (14, 16). Understanding the molecular mechanisms of tumor escape from oncogene dependence may lead to the development of more effective targeted therapeutics for cancer treatment (15, 17, 18).

Here, we demonstrate that inactivation of MYC fails to induce the complete and sustained regression of hematopoietic tumors that have lost p53 expression. Moreover, we show that this defect in tumor regression is associated with the loss of the antiangiogenic regulator thrombospondin-1 (TSP-1) (19). Restoration of either p53 or TSP-1 in p53 negative tumors was sufficient to reverse the angiogenic switch (20) and restore sustained tumor regression upon MYC inactivation. Hence, MYC inactivation combined with antiangiogenic therapy may be a previously undescribed strategy for the treatment of cancer.

Results

MYC Inactivation Induces the Sustained Regression of Specific Hematopoietic Tumors. Previously, we have described a conditional mouse model for MYC-induced tumorigenesis in hematopoietic cells. To achieve inducible and reversible MYC transgene expression, we used the tetracycline regulatory system (Tet system). To drive MYC transgene expression to the hematopoietic lineage, we used the Ig heavy chain enhancer and the SRα promoter (EμSR) (21). Using this system, MYC overexpression in hematopoietic cells occurs in the absence of doxycycline and is repressed upon addition of doxycycline to the drinking water. MYC overexpression resulted in aggressive lymphoma development (mean survival: 10 weeks; Fig. 5*A*, which is published as supporting information on the PNAS web site) (21). Continuous doxycycline treatment led to sustained MYC inactivation and resulted in the regression of tumors in all mice (21). Notably, 40% of mice remained tumor free and alive at 50 weeks (Fig. 1*A*) (21). We then investigated whether even brief MYC inactivation could induce sustained regression of primary hematopoietic tumors. MYC transgene expression was suppressed for 10 days in cohorts of transgenic mouse moribund with primary hematopoietic tumors (Fig. 1*A*). Brief inactivation of MYC expres-

Author contributions: S.G., S.R., A.C.F., P.B., A.M.K., J.F., and D.W.F. designed research; S.G., S.R., A.C.F., P.B., R.C.L., M.J.R., J.v.R., A.M.K., E.P., and F.T. performed research; S.G. and D.W.F. contributed new reagents/analytic tools; S.G., S.R., A.C.F., P.B., R.C.L., M.J.R., J.F., and D.W.F. analyzed data; and S.G., S.R., A.C.F., J.F., and D.W.F. wrote the paper.

The authors declare no conflict of interest.

Abbreviation: TSP-1, thrombospondin-1.

†Present address: Département d'Oncogenèse et Signalisation dans les Cellules Hématopoiétiques, Institut National de la Santé et de la Recherche Médicale U563, Centre de Physiopathologie Toulouse Purpan, Centre Hospitalier Universitaire Purpan, 31024 Toulouse, France.

¶Present address: Comprehensive Cancer Center, Developmental and Stem Cell Biology, University of California, San Francisco, CA 94143-0525.

‖To whom correspondence should be addressed. E-mail: dfelsher@stanford.edu.

www.pnas.org/cgi/doi/10.1073/pnas.0608017103

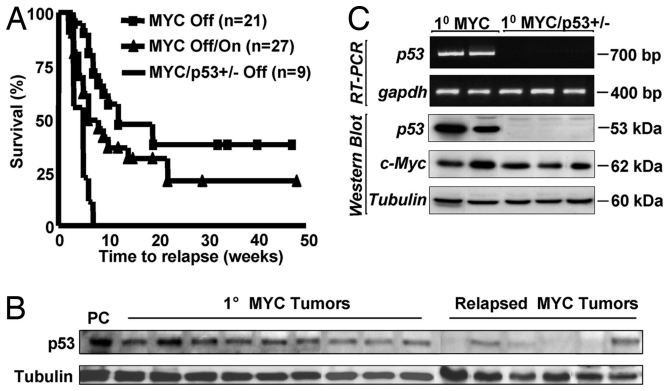

Fig. 1. Brief MYC inactivation can induce sustained tumor regression. (*A*) Kaplan–Meier plots for tumor-free survival after doxycycline treatment (100 μg/ml). The genotypes of the mice and the sustained (MYC Off) or brief (MYC Off/On) MYC inactivation are indicated. The number of mice in each group is denoted by the *n* values. Primary tumor regression and relapse were monitored for up to 50 weeks. Statistical comparison of Kaplan–Meier plots is based on the log-rank test. (*B*) p53 protein expression levels in MYC primary and relapsed tumors. Western blot analysis was performed on protein lysates prepared from MYC primary and relapsed tumors. Equal loading was confirmed by anti-α tubulin Western blot analysis. PC, positive control. (*C*) p53 protein and mRNA expression in primary (10) MYC versus primary MYC/p53$^{+/-}$ tumors. PCR was performed to measure p53 and gapdh mRNA. Western blot analysis of p53, MYC, and tubulin protein expression were performed.

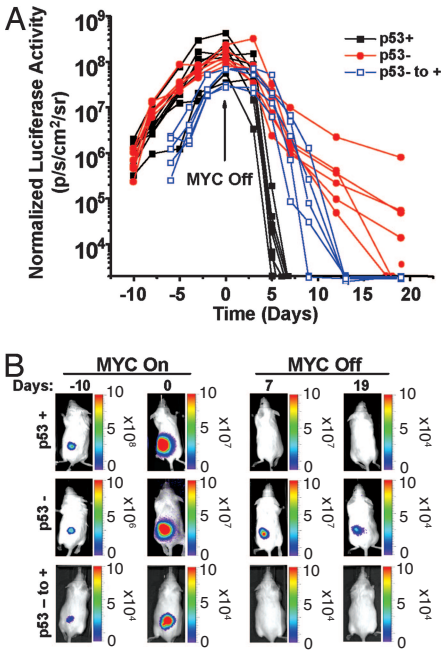

Fig. 2. p53 status and the rate of tumor cell elimination upon MYC inactivation. (*A*) Measurement of tumor cell elimination upon MYC inactivation. p53 wild-type (p53^{+}), p53 negative (p53^{-}), and p53 restored (p53^{-} to $^{+}$) tumor cells were retrovirally labeled with luciferase before s.c. injection into syngeneic mice. Mice were serially imaged by bioluminescence imaging at the indicated times, before and after MYC inactivation, to monitor transplanted tumor growth (MYC On) and tumor regression upon doxycycline treatment (100 μg/ml) (MYC Off). A summary of changes in luciferase activity is shown. Each cohort consisted of at least 5 mice. Representative data from one of three experiments is shown. (*B*) Representative images of bioluminescence imaging.

sion also was sufficient to induce sustained tumor regression and 20% of transgenic mice survived for as long as 50 weeks (Fig. 1*A*). No significant difference ($P = 0.1957$) was observed comparing survival upon sustained or brief MYC inactivation (Fig. 1*A*). When brief MYC inactivation was performed on secondary transplanted tumors into syngeneic hosts, we observed sustained tumor regression in three of four tumors (relapse rate versus injected mice: 2/4, 0/7, 0/5, or 0/7). Therefore, the ability of MYC inactivation to induce complete and sustained tumor regression appears to reflect an intrinsic tendency of each tumor.

Loss of p53 Function Facilitates Tumor Relapse. Loss of p53 function is common in tumors (22) and has been described to play a critical role in tumor recurrence (13). Therefore, we analyzed whether p53 loss would promote tumor relapse after MYC inactivation in our lymphoma model. Consistent with this possibility, primary lymphoid tumors that had relapsed after MYC inactivation often demonstrated loss of p53 expression (Fig. 1*B*). To directly investigate the effect of loss of p53 function, cohorts of mice that expressed a conditional MYC transgene in concert with the loss of one p53 allele were generated. Similar to previous reports (23–26), the loss of one p53 allele was sufficient to accelerate tumorigenesis with a reduction in the mean latency of tumor onset by 3 weeks (Fig. 5*A*, $P < 0.0001$). Primary tumors induced by the conditional MYC transgene expressed p53 mRNA and protein, whereas primary tumors arising from mice genetically heterozygous for p53, had lost p53 mRNA and protein expression, that could in some cases be explained by the loss of the second p53 allele (Figs. 1*C* and 5*B*).

The primary p53 negative tumors initially all regressed upon sustained MYC inactivation, and the mice clinically recovered, but these tumors always relapsed, in contrast to primary p53 wild-type tumors (Fig. 1*A*, $P = 0.0002$; Fig. 2). There are several possible explanations for our results. First, it was possible that loss of p53 function facilitated the ability of tumors to either bypass the Tet system and express the MYC transgene or activate expression of endogenous C-, N- or L-Myc. However, when relapsed tumors were examined for MYC protein expression, overexpression of the human MYC transgene or endogenous C-, N-, or L-Myc proteins was not observed (Fig. 6, which is published as supporting information on the PNAS web site). Thus, the relapsed tumors had become independent of MYC expression, similar to what we have described (6).

Another possibility was that tumors arising in the context of MYC overexpression and loss of p53 expression were different types of lymphomas that may account for their different response to MYC inactivation. Although this possibility cannot be excluded, the tumors induced by MYC overexpression versus MYC overexpression and loss of p53 exhibited similar histology and identical FACS phenotype: Thy-1, CD4, CD8, CD3, CD5, and T cell antigen receptor $\alpha\beta$ positive (data not shown). Another possibility is that loss of p53 induced genomic destabilization facilitating the ability of tumors to acquire genetic events that could compensate for loss of MYC overexpression. However, we have previously performed spectral karyotype analysis of tumors and failed to detect differences in genomic abnormalities in p53 positive versus negative tumors (6). A final possibility was that p53 loss allowed tumors to escape their dependence upon MYC overexpression by preventing the elimination of tumor cells.

p53 Loss Impairs the Eradication of Tumor Cells upon MYC Inactivation. To precisely evaluate how loss of p53 function influences tumor regression upon MYC inactivation, we used bioluminescence imaging (27) to compare the kinetics of transplanted p53 positive and negative tumor elimination upon MYC inactivation *in vivo*. We retrovirally introduced the luciferase enzyme into tumor-derived cell lines. The luciferase-labeled cells were detected with a minimal sensitivity of 1,000 cells per site and over a multiple log range in cell number (data not shown). Cohorts of mice were inoculated s.c. with luciferase-labeled p53-positive or -negative tumors and the intensity of the luminescent signal was monitored before and after MYC

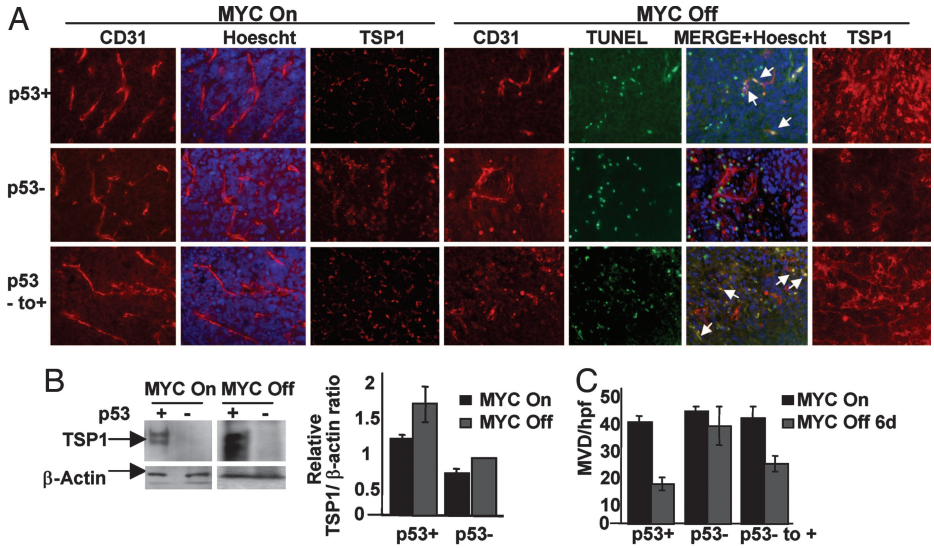

Fig. 3. p53 status modifies the angiogenic response of tumors upon MYC inactivation. (*A Left*) p53 status does not affect the angiogenic response of tumor onset upon MYC activation. p53 wild-type ($p53^+$), p53 negative ($p53^-$) and p53 restored ($p53^-$ to $^+$) transplanted tumors were examined by immunofluorescence for microvessel density (CD31) and TSP-1 expression (MYC on). (*A Right*) The loss of p53 decreases TSP-1 levels despite MYC inactivation. p53 wild-type ($p53^+$), p53 negative and p53 restored ($p53^-$ to $^+$) transplanted tumors were examined by immunofluorescence for microvessel density (CD31) and TSP-1 expression 6 days after MYC inactivation (MYC Off). Whereas there was no significant difference in the level of TUNEL reactivity, there were significantly more TUNEL-positive endothelial cells (white arrow) in p53 wild-type ($p53^+$) and p53 restored ($p53^-$ to $^+$) tumors as compared with p53 negative ($p53^-$) tumors. Specificity of staining was ensured by immunostaining of serial tumor sections with isotype matched control antibodies. (*B*) Western blot analysis of p53 wild-type ($p53^+$) and p53 negative ($p53^-$) transplanted tumors were performed for TSP-1 expression upon MYC activation and 6 days after MYC inactivation. Densitometric analysis demonstrated significantly higher TSP-1 expression in p53 wild-type ($p53^+$) tumor cells relative to β-actin as compared with p53 negative ($p53^-$) tumor cells. (*C*) Quantification of microvessel density (MVD) per high power field (hpf) demonstrated significantly increased MVD/hpf in p53 negative ($p53^-$) tumors 6 days after MYC inactivation as compared with p53 wild-type ($p53^+$) tumors. At least five fields were counted in representative tumor sections, and at least two different transplanted tumors were analyzed. Values are represented as means ± standard deviation.

inactivation to measure kinetics of tumor regression (Fig. 2*A*). The initial rate of tumor regression was similar in $p53^+$ and $p53^-$ tumors within the first 2 days of MYC inactivation and the first log in tumor reduction (Fig. 2). However, after 2 days, $p53^+$ tumors were rapidly eliminated, whereas $p53^-$ tumors continued to persist in the host after MYC inactivation. After 19 days of MYC inactivation, a bioluminescent signal was detected in mice injected with $p53^-$ tumor cells, whereas complete tumor elimination was observed in mice injected with $p53^+$ tumor cells (Fig. 2). Thus, the loss of p53 had no effect on the initial consequences of MYC inactivation but prevented the complete eradication of tumor cells.

p53 Loss Blocks a TSP-1-Mediated Antiangiogenic Response upon MYC Inactivation. Angiogenesis is critical for the expansion of tumor mass (28). The MYC oncogene has been shown to regulate angiogenesis and specifically inhibit the expression of the antiangiogenesis regulator TSP-1 (29–32). Conversely, p53 has been described to suppress tumor angiogenesis and also has been shown to regulate TSP-1 (33, 34). Hence, we speculated that the loss of p53 might impede complete tumor regression upon MYC inactivation by blocking the antiangiogenic response mediated via TSP-1. Transplanted p53 positive and negative tumors were examined by immunofluorescence for microvessel density (CD31) and TSP1 expression, at tumor onset and 6 days after MYC inactivation (Fig. 3 *A* and *B*). Whereas p53 status did not affect CD31 or TSP-1 expression during tumor onset (Fig. 3*A*, MYC On), striking differences in TSP-1 expression were observed upon MYC inactivation (Fig. 3*A*, MYC Off). Importantly, $p53^-$ tumors exhibited significantly lower levels of TSP-1 expression despite MYC inactivation. Reduced TSP-1 expression in $p53^-$ tumor cells was also confirmed by Western blot analysis (Fig. 3*B*). To further confirm that p53 loss influenced the angiogenic program upon MYC inactivation, tumor microvessel density was evaluated by performing endothelial cell specific CD31 staining. Even six days after MYC inactivation, we noticed the persistence of larger lumen vessels in p53 deficient tumors whereas $p53^+$ tumors exhibited reduced CD31 staining (Fig. 3*A*). Using TUNEL analysis, we observed endothelial cell apoptosis in $p53^+$, but not $p53^-$ tumors upon MYC inactivation. Furthermore, before MYC inactivation, microvessel density (MVD) was found to be similar in $p53^+$ and $p53^-$ tumors. However, after MYC inactivation, $p53^+$, but not $p53^-$ tumors, exhibited a significant reduction in MVD (Fig. 3*C*). Together these data suggest that $p53^-$ tumors failed to induce sufficient levels of TSP-1 to mediate the appropriate antiangiogenic response to MYC inactivation necessary for complete and sustained tumor regression.

Restoration of p53 Permits Sustained Tumor Regression upon MYC Inactivation. Loss of p53 resulted in a defect in tumor regression by preventing angiogenesis inhibition induced by MYC inactivation. We reasoned that by restoring p53, we would induce a more complete antiangiogenic response and subsequently sustain tumor regression upon MYC inactivation. To investigate the consequences of p53 restoration, three different $p53^-$ tumor derived cell lines (6814, 7031, and B-1601) were retrovirally transduced with p53. Importantly, the level of p53 protein expression was found to be comparable to several tumor-derived cell lines positive for p53, as measured by Western blot analysis (Fig. 7, which is published as supporting information on the PNAS web site).

We then investigated whether p53 restoration would rescue TSP-1 expression and decrease tumor neovascularization. TSP-1 and CD31 levels were examined in transplanted p53 restored ($p53^-$ to $^+$) tumor specimens isolated 6 days after MYC inactivation. Ectopic expression of p53 led to restoration of TSP-1 levels comparable to $p53^+$ tumors upon MYC inactivation (Fig. 3*A*). In addition, CD31 and TUNEL staining revealed both increased endothelial cell apoptosis and reduced microvessel density in p53 restored ($p53^-$ to $^+$) tumors (Fig. 3 *A* and *C*).

Finally, we examined the influence of p53 restoration on the

kinetics of tumor cell elimination *in vivo* upon MYC inactivation by bioluminescence imaging. We found that transplanted p53 restored tumors exhibited rapid and complete tumor cell elimination comparable to $p53^+$ tumors (Fig. 2). Thus, restoration of p53 now permitted complete tumor cell elimination upon MYC inactivation *in vivo*.

Restoration of Either TSP-1 or p53 Is Associated with Sustained Tumor Regression upon MYC Inactivation. Next we examined whether TSP-1 restoration alone could maintain tumor regression upon MYC inactivation even with the loss of p53. $p53^+$, $p53^-$, p53 restored, or $p53^-/TSP\text{-}1^{HI}$ tumor cells were inoculated s.c. into syngeneic hosts and mice were treated with doxycycline. $TSP\text{-}1^{HI}$ expression was achieved in $p53^-$ tumor cells through serial retroviral transduction. TSP-1 expression was confirmed by quantification of Western analysis and immunohistochemical staining and demonstrated similar expression levels as in $p53^+$ tumors (Fig. 8, which is published as supporting information on the PNAS web site). Whereas restoration of TSP-1 expression did not influence the kinetics of transplanted tumor growth, similar to restoration of p53, transplanted $p53^-/TSP\text{-}1^{HI}$ tumor cells were eliminated rapidly and more completely as compared with transplanted $p53^-$ tumor cells (Fig. 4*A*, $P < 0.03$). Further, transplanted tumors with $TSP\text{-}1^{HI}$ expression were associated with decreased CD31 staining and MVD (Fig. 8).

Finally, we examined whether p53 or TSP-1 restoration could prevent tumor relapse upon MYC inactivation. $p53^-$ or p53 restored tumor cells were inoculated i.p. into syngeneic hosts and mice were treated with doxycycline at tumor onset. As expected, after initial tumor regression, transplanted $p53^-$ tumors relapsed rapidly, with a mean relapse time of 5.5 weeks after MYC inactivation. However, transplanted p53 restored tumors exhibited a significant delay until tumor relapse ranging from 6 to 37 weeks (Fig. 4*B*, $P < 0.0001$) with 3 mice exhibiting sustained tumor regression even after 37 weeks. Similarly, transplanted TSP-1 restored tumors ($TSP\text{-}1^{HI}$) exhibited prolonged survival (Fig. 4*C*, $P = 0.0122$). Notably, the transplanted tumors that relapsed in the p53 restored cohort had lost p53 protein expression, as seen by Western blot analysis (Fig. 4*D*), with one exception (R4), which expressed higher levels of a most likely mutated p53 allele. Hence, the sustained restoration of p53 expression in tumors significantly enhanced the ability of MYC inactivation to induce sustained tumor regression. Thus, the restoration of either p53 or TSP-1 expression in $p53^-$ tumors is sufficient to permit tumor regression and to limit tumor relapse upon MYC inactivation.

Discussion

We found that the loss of p53 function prevents sustained tumor regression upon MYC inactivation corresponding with the loss of induction of the antiangiogenic regulator, TSP-1 and the suppression of tumor angiogenesis. Furthermore, the restoration of either p53 or TSP-1 in p53 negative tumor cells now permitted MYC inactivation to induce the shut off of the angiogenic switch and sustained tumor regression. Importantly, overexpression of TSP-1 alone did not influence tumor growth suggesting that only a combination of MYC inactivation and TSP-1 expression was sufficient to induce tumor regression. Hence, angiogenesis appears to be an essential component of oncogene addiction.

We have gained some critical insight into the mechanism of tumor regression upon MYC inactivation. Previously, we described that MYC inactivation induced cell autonomous proliferative arrest and apoptosis of hematopoietic tumor cells. Here we have demonstrated that MYC inactivation in hematopoietic tumors also appears to require a blockade in tumor angiogenesis. Furthermore, we demonstrate that p53 is required for a TSP-1 mediated antiangiogenic response upon MYC inactivation. Therefore, MYC inactivation appears to induce tumor regression at least in part through a p53-dependent induction of TSP-1 expression. Future studies should address whether in epithelial tumor models p53 similarly regulates TSP-1 expression.

Our results are consistent with previous studies that have suggested that MYC (29–32) or p53 (33–36) may be involved in the

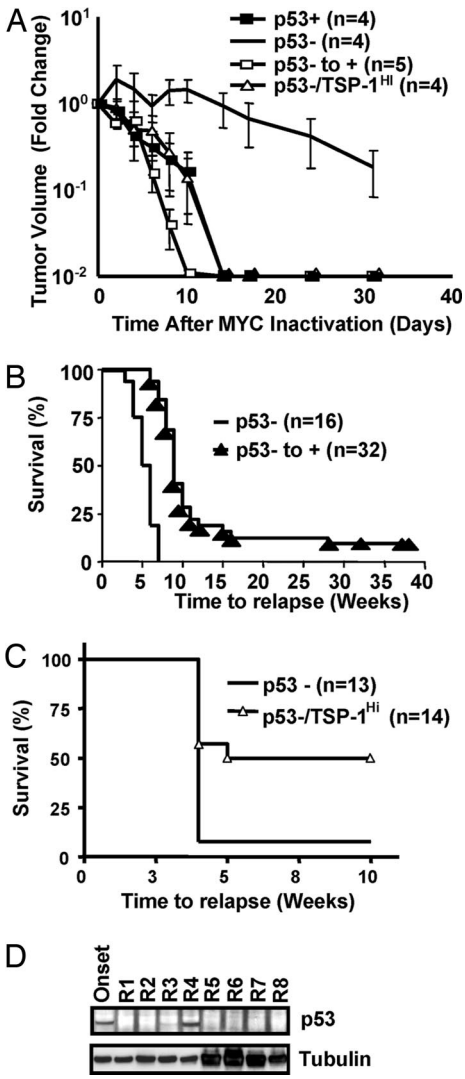

Fig. 4. Combined inactivation of MYC and restoration of p53 or TSP-1 expression is more effective in inducing tumor regression. (*A*) Restoration of p53 or TSP-1 and tumor regression upon MYC inactivation. In these experiments, p53 or TSP-1 was transduced into tumor cells and maintained under continuous selection *in vitro* to ensure expression. p53 positive ($p53^+$), p53 negative ($p53^-$), p53 restored ($p53^-$ to $^+$) and p53-/$TSP\text{-}1^{HI}$ tumor cells were injected s.c. at a dose of 10^7 cells into cohorts of syngeneic FVB/N-recipient mice. When transplanted tumors reached 2 cm^2 in size, mice were treated with doxycycline (100 μg/ml) to inactivate MYC. Tumor volume is calculated from caliper measurement and is expressed as logarithmic fold changes in tumor volume before MYC inactivation. Data are presented as the mean for each cohort ± SEM with statistical analysis performed by the Mann–Whitney test. (*B* and *C*) MYC inactivation, combined with p53 or TSP-1 restoration, delays tumor relapse *in vivo*. p53 negative ($p53^-$), p53 restored ($p53^-$ to $^+$), or TSP-1 restored (p53-/$TSP\text{-}1^{HI}$) cells (10^7) were injected i.p. into syngeneic mice. When moribund with tumor burden, transplanted mice were treated with doxycycline (100 μg/ml) and monitored for tumor relapse. Kaplan–Meier survival curve are represented. Statistical comparison of Kaplan–Meier plots is based on the log-rank test. The number of mice in each group is denoted by *n* values. (*D*) Tumor relapse after MYC inactivation is frequently associated with reduced p53 protein expression. p53 expression levels in p53 restored tumor cells, at the time of tumor onset and relapse (R1–R8), was analyzed by Western blot on protein lysates (60 μg) prepared from transplanted relapsed tumor tissues. Protein loading was assayed by anti-α-tubulin Western blot.

regulation of tumor angiogenesis and that TSP-1 is a negative regulator of tumorigenesis (37, 38). This study illustrates that MYC inactivation requires either p53 or TSP-1 to inhibit angiogenesis and induce sustained tumor regression. Importantly, we demonstrate that tumor relapse due to the loss of p53 can be significantly delayed or even prevented, in some cases, by restoration of TSP-1 expression to maintain tumor regression after MYC inactivation.

Our results may be more generally relevant to the mechanisms by which targeted therapeutics induce tumor regression. The restoration of either p53 or TSP-1 may be similarly effective in permitting sustained tumor regression upon oncogene inactivation in other tumor models (11–13). In this context, it will be interesting to determine whether TSP-1 expression is systematically induced upon oncogene inactivation, regardless of the specific oncogene and cancer type (39). In addition, it will be important to determine whether tumor relapse after oncogene inactivation is associated with TSP-1 loss, especially in p53 wild-type tumors.

Human tumors are generally considered to be more complex than mouse tumors and targeting any single mutant gene product is unlikely to be sufficient to induce durable tumor regression. In this regard, it has been recently illustrated that the loss of p53 or p19ARF impairs the ability of Imatinib to regress BCR-ABL induced tumors through unknown mechanisms (40, 41). The restoration of p53 or p19ARF may enhance the clinical response of human tumors to Imatinib; and possibly this may occur through regulation of angiogenesis. Our results provide one illustration where the combined inactivation or repair of multiple gene products and/or pathways such as the inactivation of an oncogene, MYC, plus the restoration of a tumor suppressor, p53, or a regulator of angiogenesis, TSP-1, is more likely to be effective in the treatment of cancer. Generally, our results support the idea that the combined inactivation of an oncogene and the inhibition of angiogenesis will be an effective therapeutic strategy for cancer.

Materials and Methods

Transgenic Mice. The generation and characterization of Tet system transgenic lines for conditional expression of MYC, have been described (21). p53 knockout mice were kindly provided by Alan Bradley (Baylor University, Houston, TX) and were generously provided in the FVB/N background by Lisa Coussens (University of California, San Francisco). Genotyping was performed by PCR on genomic DNA from tails. Analysis of the p53 wild-type or mutated allele was performed as described (42). Animals were housed in the Stanford vivarium as per animal protocols approved by Stanford University.

Tumor Surveillance and Tumorigenicity Assays. Transgenic mice were observed biweekly for tumor development. When mice were moribund with tumor burden, they were either humanely euthanized or treated with doxycycline in their drinking water (100 μg/ml) to follow tumor regression and relapse. Percent survival of MYC overexpressing mice with or without p53 loss was measured as the mice life duration and used to assess lymphomagenesis. To monitor for tumor regression and relapse, percent survival was measured as the time between doxycycline treatment (if tumor regression occurred within 1 week) and relapse, which is defined as recurrence of signs of morbidity. Statistical comparison of Kaplan–Meier curves is based on the log-rank test. For transplantation experiments, primary tumors were first adapted to *in vitro* growth as described (21) and then 10^7 cells were washed once in PBS before i.p. or s.c. injection into FVB/N syngeneic mice. To assess for tumor regression, transplanted s.c. tumors were measured by using a caliper over a 30-day period of doxycycline treatment, and tumor volumes were calculated by using the formula length (mm) $\times$ width^2 (mm) $\times$ 0.52 (20, 43).

Cell Culture. Tumor-derived cell lines were generated by mechanical disruption of tumor tissue followed by Ficoll–Paque purification of the single cell suspension. Cells were then maintained *in vitro* as described (21). To inactivate human c-MYC transgene expression, tumor cells were treated with doxycycline at 20 ng/ml.

Retrovirus Constructs, Virus Production and Tumor Cell Infection. MSCV-IRES-GFP and MSCV-p53-IRES-GFP constructs were kindly provided by S. Lowe (Cold Spring Harbor Laboratory, Cold Spring Harbor, NY). MSCV-LUC-IRES-GFP construct was kindly provided by Luis Soares (Stanford University). MSCV-Puro-LUC construct, a modified version of the pDON plasmid vector (Takara Mirus Bio, Madison, WI), was kindly provided by Mobin Karimi and Robert Negrin (Stanford University). Retroviruses containing supernatants were prepared by transient transfection of 293T cells, and viral titers were measured as described (44). Tumor cells were incubated with retroviruses containing supernatants for 12 h at 32°C in media containing 4 μg/ml polybrene. Cells were then expanded at 37°C for an additional 48 h and GFP expressing cells were purified by flow cytometry on a FACS Vantage (Becton Dickinson, Franklin Lakes, NJ). Cells containing MSCV-Puro-LUC were selected with puromycin.

TSP-1 retrovirus was produced by transfecting GPG-293 cells with 8 μg of PWZL-TSP1 plasmid DNA or PWZL vector alone (Addgene, Cambridge, MA) and 24 μl of Mirus TransIT Express transfection reagent. High-titer viral supernatant was collected at days 5, 7, and 9 after transfection. Virus was concentrated by high-speed centrifugation, and used to infect 2×10^5 p53$^-$ cells by spin-infection at 2,000 $\times$ *g* for 2 h with vector alone or serially incubated with TSP-1 virus three times.

***In Vivo* Bioluminescence Imaging.** p53 wild-type (p53$^+$), p53 negative (p53$^-$) and p53 restored (p53$^-$ to $^+$) tumor cells, expressing the luciferase enzyme, were injected i.p. or s.c. into syngeneic mice. Tumors were allowed to develop until reaching a similar bioluminescent signal. Tumor regression was then induced by doxycycline treatment (100 μg/ml). Mice developing transplanted tumors were anesthetized with a combination of inhaled isoflorane/oxygen delivered by the Xenogen XGI-8 5-port Gas Anesthesia System. The substrate D-luciferin (150 mg/kg) was injected into the animal's peritoneal cavity 10 min. before imaging. Animals were then placed into a light-tight chamber and imaged with an IVIS-100 cooled CCD camera (Xenogen, Alameda, CA). First, a grayscale body surface reference image (digital photograph) was taken under weak illumination. Next, photons emitted from luciferase expressing cells within the animal and transmitted through the tissues were collected for a period of 5 sec to 1 min and quantified by the software program Living Image (Xenogen) as an overlay on the image analysis program "Igor" (Wavemetrics, Seattle, WA). For anatomical localization, a pseudocolor image representing light intensity (blue, least intense; red, most intense) was generated in Living Image and superimposed over the gray scale whole body reference image as described previously (45). Living Image was used to collect, archive, and analyze photon fluxes and transform them into pseudocolor images by using Living Image software (Xenogen). At least 5 mice per group were injected with tumors expressing luciferase.

Immunohistochemistry. Mice were euthanized at tumor onset and 6 days after MYC inactivation, and transplanted tumors were harvested and fixed in neutral buffered formalin for paraffin sections. Paraffin embedded tumor sections were deparaffinized by successive incubations in xylene, 95% ethanol, 90% ethanol, 70% ethanol followed by PBS. Epitopes were unmasked with 20 ug/ml proteinase K in PBS at room temperature for 30 min and rinsed twice in PBS plus 0.3% Triton X-100 (PBS-T). Sections were immunostained with rat anti-CD31 mAb (1:50; Pharmingen, San Diego, CA), mouse anti-TSP1 (clone A6.1, 1:50; Lab Vision, Fremont, CA), or an isotype matched control (Pharmingen) overnight at room temperature. This was followed by incubation for 2 h with

goat anti-rat Alexa 594 or goat anti-mouse Alexa 594 conjugated secondary antibody (1:500; Molecular Probes). Nuclei were labeled by brief washes in Hoechst dye (Sigma, St. Louis, MO; 1 ug/ml).

For TUNEL staining, after anti-CD31 immunostaining, sections were stained by using the DeadEnd Fluorometric TUNEL System (Promega). In brief, sections were incubated for 15 min in equilibration buffer followed by incubation with nucleotide mix (containing fluorescein-12-dUTP) and terminal deoxynucleotidyl transferase enzyme for 60 min at 37°C. Reactions were stopped by incubation in 2× SSC for 15 min followed by serial washes in PBS-T. Sections were mounted with glycerol, and images were obtained on a Zeiss microscope and analyzed by using AxioVision 4.0 software (Carl Zeiss Vision).

Western Blot Analysis. Tumor pieces or tumor-derived cell lines were lysed in Tris·HCl, pH 8/50 mM/NaCl 150 mM/1% Triton X-100/DTT 1 mM/1× inhibitor mixture mix (Calbiochem, San Diego, CA)/100 μg/ml PMSF. Western blots were performed on protein lysates (60 μg) by using conventional techniques. p53 protein expression was detected by using antibodies obtained from Novocastra Laboratories at a dilution of 1/400. As a positive control for p53 expression, a lysate prepared from MEF cells that overexpress p53 was used (46). MYC protein levels were assessed by using human c-MYC (9E10, Oncogene, San Diego, CA) (dilution 1/200), mouse c-Myc (c19; Santa Cruz Biotechnology, Santa Cruz, CA) (dilution 1/250), mouse N-Myc (OP13; Oncogene) (dilution 1/100), and mouse L-Myc (c20; Santa Cruz Biotechnology) (dilution 1/100) antibodies. As a positive control for N-Myc and L-Myc, protein lysates were prepared from BJAB cells (Santa Cruz Biotechnology) and NCI-H209 cells (American Type Culture Collection Biotechnology, Manassas, VA), respectively. The α-tubulin antibodies were purchased from Oncogene (Ab-1) and used at a dilution of 1/500. Horseradish peroxidase (HRP)-coupled secondary antibodies were obtained from Amersham Biosciences and used at a dilution of 1/2,000. Protein bands were visualized by using the ECL1$^+$ detection kit (Amersham Biosciences, Piscataway, NJ). Expression of TSP-1 was assessed by immunoblotting whole-cell lysates. Cells were treated for 10 h with doxycycline in RPMI media alone, washed three times with PBS, and then lysed with sample buffer. Cells (1×10^6) were loaded on a 6% Tris·HCl SDS/PAGE gel, subjected to gel electrophoresis, and transferred to a nitrocellulose membrane. The membrane was incubated with TSP-1 mAb (Neomarker Ab-11; 1/1,000) in TBST for 1 h at room temperature, then washed and incubated with goat anti-mouse HRP (Zymed; 1/1,000). Protein bands were visualized with the ECL detection kit (Amersham). Membranes were stripped and reprobed with anti-β-actin mAb (1/5,000) followed by goat anti-mouse HRP and visualized by ECL detection. Films were densitometrically analyzed, and TSP-1 levels were normalized to β-actin levels.

Microvessel Density. Transplanted tumors were harvested 6 days after MYC inactivation and paraffin embedded. Microvessel density was determined by immunofluorescence staining of deparaffinized tumor sections with an anti-CD31 mAb (PharMingen; 1/50) overnight at room temperature followed by a Goat anti-rat Alexa 594 (Molecular Probes; 1/500) for 2 h at room temperature. Sections were briefly rinsed with Hoechst dye to stain nuclei. By following the method as described (47), at low magnification (×40), regions of highest vessel density were captured and counted at ×200 magnification (0.738 mm^2 field). At least five fields were counted in a representative tumor section, and at least two different transplanted tumors were counted. Values are represented as means ± SD.

This work is dedicated in memory of Mr. Georges Guedj. We thank Drs. Michael Cleary, Laura Attardi, Steven Artandi, Mark Lee, and members of the D.W.F. laboratory for helpful discussions and a critical reading of the manuscript, Dr. Jack Lawler for helpful advice, and Randolph Watnick for helpful discussions. This work was supported by a postdoctoral fellowship from the Lymphoma Research Foundation (to S.G.); the Richard and Susan Smith Family Foundation (to S.R.); the Leukemia and Lymphoma Society Career Development Special Fellow in Clinical Research Award (to A.F.); the Stanford Medical Scholars Program (to P.B.); the Howard Hughes Medical Institute Medical Student Research Fellowship (to A.K.); a postdoctoral fellowship from the Jose Carreras Leukemia Foundation (to E.P.); the Breast Cancer Research Foundation (to J.F.); and National Cancer Institute (NCI) Grants R01-CA85610, R01-CA105102, 3R01CA089305-03S1; National Institutes of Health (NIH)/NCI *In Vivo* Cellular and Molecular Imaging Center Grant P50; NIH/NCI Grant 1P20 CA112973; the Leukemia and Lymphoma Society; the Burroughs Wellcome Fund; and the Damon Runyon Lilly Clinical Investigator Award (to D.W.F.).

1. Bishop JM (1991) *Cell* 64:235–248.
2. Hahn WC, Weinberg RA (2002) *N Engl J Med* 347:1593–1603.
3. Sawyers CL (2002) *Cancer Cell* 1:13–15.
4. Felsher DW (2003) *Nat Rev Cancer* 3:375–379.
5. Giuriato S, Rabin K, Fan AC, Shachaf CM, Felsher DW (2004) *Semin Cancer Biol* 14:3–11.
6. Karlsson A, Giuriato S, Tang F, Fung-Weier J, Levan G, Felsher DW (2003) *Blood* 101:2797–2803.
7. Jain M, Arvanitis C, Chu K, Dewey W, Leonhardt E, Trinh M, Sundberg CD, Bishop JM, Felsher DW (2002) *Science* 297:102–104.
8. Shachaf CM, Kopelman AM, Arvanitis C, Karlsson A, Beer S, Mandl S, Bachmann MH, Borowsky AD, Ruebner B, Cardiff RD, *et al.* (2004) *Nature* 431:1112–1117.
9. Weinstein IB (2002) *Science* 297:63–64.
10. Jonkers J, Berns A (2004) *Cancer Cell* 6:535–538.
11. D'Cruz CM, Gunther EJ, Boxer RB, Hartman JL, Sintasath L, Moody SE, Cox JD, Ha SI, Belka GK, Golant A, *et al.* (2001) *Nat Med* 7:235–239.
12. Giuriato S, Felsher DW (2003) *Cell Cycle* 2:329–332.
13. Gunther EJ, Moody SE, Belka GK, Hahn KT, Innocent N, Dugan KD, Cardiff RD, Chodosh LA (2003) *Genes Dev* 17:488–501.
14. Shah NP, Nicoll JM, Nagar B, Gorre ME, Paquette RL, Kuriyan J, Sawyers CL (2002) *Cancer Cell* 2:117–125.
15. Shah NP, Tran C, Lee FY, Chen P, Norris D, Sawyers CL (2004) *Science* 305:399–401.
16. Gorre ME, Mohammed M, Ellwood K, Hsu N, Paquette R, Rao PN, Sawyers CL (2001) *Science* 293:876–880.
17. Tipping AJ, Baluch S, Barnes DJ, Veach DR, Clarkson BM, Bornmann WG, Mahon FX, Goldman JM, Melo JV (2004) *Leukemia* 18:1352–1356.
18. Wendel HG, De Stanchina E, Fridman JS, Malina A, Ray S, Kogan S, Cordon-Cardo C, Pelletier J, Lowe SW (2004) *Nature* 428:332–337.
19. Rodriguez-Manzaneque JC, Lane TF, Ortega MA, Hynes RO, Lawler J, Iruela-Arispe ML (2001) *Proc Natl Acad Sci USA* 98:12485–12490.
20. Hanahan D, Folkman J (1996) *Cell* 86:353–364.
21. Felsher DW, Bishop JM (1999) *Mol Cell* 4:199–207.
22. Soussi T, Beroud C (2001) *Nat Rev Cancer* 1:233–240.
23. Blyth K, Terry A, O'Hara M, Baxter EW, Campbell M, Stewart M, Donehower LA, Onions DE, Neil JC, Cameron ER (1995) *Oncogene* 10:1717–1723.
24. Elson A, Deng C, Campos-Torres J, Donehower LA, Leder P (1995) *Oncogene* 11:181–190.
25. Eischen CM, Weber JD, Roussel MF, Sherr CJ, Cleveland JL (1999) *Genes Dev* 13:2658–2669.
26. Yu D, Thomas-Tikhonenko A (2002) *Oncogene* 21:1922–1927.
27. Edinger M, Cao YA, Hornig YS, Jenkins DE, Verneris MR, Bachmann MH, Negrin RS, Contag CH (2002) *Eur J Cancer* 38:2128–2136.
28. Folkman J (2002) *Semin Oncol* 29:15–18.
29. Baudino TA, McKay C, Pendeville-Samain H, Nilsson JA, Maclean KH, White EL, Davis AC, Ihle JN, Cleveland JL (2002) *Genes Dev* 16:2530–2543.
30. Brandvold KA, Neiman P, Ruddell A (2000) *Oncogene* 19:2780–2785.
31. Janz A, Sevignani C, Kenyon K, Ngo CV, Thomas-Tikhonenko A (2000) *Nucleic Acids Res* 28:2268–2275.
32. Watnick RS, Cheng YN, Rangarajan A, Ince TA, Weinberg RA (2003) *Cancer Cell* 3:219–231.
33. Browder T, Folkman J, Hahnfeldt P, Heymach J, Hlatky L, Kieran M, Rogers MS (2002) *Science* 297:471, discussion 471.
34. Dameron KM, Volpert OV, Tainsky MA, Bouck N (1994) *Cold Spring Harb Symp Quant Biol* 59:483–489.
35. Hammond EM, Giaccia AJ (2002) *Science* 297:471, discussion 471.
36. Yu JL, Rak JW, Coomber BL, Hicklin DJ, Kerbel RS (2002) *Science* 295:1526–1528.
37. Lawler J (2002) *J Cell Mol Med* 6:1–12.
38. Sund M, Hamano Y, Sugimoto H, Sudhakar A, Soubasakos M, Yerramalla U, Benjamin LE, Lawler J, Kieran M, Shah A, Kalluri R (2005) *Proc Natl Acad Sci USA* 102:2934–2939.
39. Folkman J, Ryeom S (2005) *Cold Spring Harbor Symp Quant Biol* 70:389–397.
40. Wendel HG, de Stanchina E, Cepero E, Ray S, Emig M, Fridman JS, Veach DR, Bornmann WG, Clarkson B, McCombie WR, *et al.* (2006) *Proc Natl Acad Sci USA* 103:7444–7449.
41. Williams RT, Roussel MF, Sherr CJ (2006) *Proc Natl Acad Sci USA* 103:6688–6693.
42. Donehower LA, Harvey M, Slagle BL, McArthur MJ, Montgomery CA, Jr., Butel JS, Bradley A (1992) *Nature* 356:215–221.
43. Kuo CJ, Farnebo F, Yu EY, Christofferson R, Swearingen RA, Carter R, von Recum HA, Yuan J, Kamihara J, Flynn E, *et al.* (2001) *Proc Natl Acad Sci USA* 98:4605–4610.
44. Pear WS, Nolan GP, Scott ML, Baltimore D (1993) *Proc Natl Acad Sci USA* 90:8392–8396.
45. Contag CH, Spilman SD, Contag PR, Oshiro M, Eames B, Dennery P, Stevenson DK, Benaron DA (1997) *Photochem Photobiol* 66:523–531.
46. Jimenez GS, Nister M, Stommel JM, Beeche M, Barcarse EA, Zhang XQ, O'Gorman S, Wahl GM (2000) *Nat Genet* 26:37–43.
47. Weidner N, Semple JP, Welch WR, Folkman J (1991) *N Engl J Med* 324:1–8.